EFFECT OF HARDENING AND DAMAGE PARAMETERS ON THE PREDICTION OF LOCALIZED NECKING IN THIN SHEET METALS

Yasser Bouktir[1,2(*)], Hocine Chalal[1,3], Farid Abed-Meraim[1,3]

[1]Laboratoire d'Étude des Microstructures et de Mécanique des Matériaux, Arts et Métiers ParisTech, Metz, France
[2]Laboratoire Procédés de Fabrication, École Militaire Polytechnique, Bordj El Bahri, Algeria
[3]Laboratory of Excellence on Design of Alloy Metals for low-mAss Structures, DAMAS, Université de Lorraine, France
(*)*Email:* Yasser.BOUKTIR@ensam.eu

ABSTRACT

In this work, an elastic–plastic model with Hill'48 anisotropic yield surface is coupled with the continuum damage mechanics theory and combined with the bifurcation analysis, in order to predict strain localization in thin sheet metals. The resulting approach is implemented into the ABAQUS finite element code within the framework of large strains and plane-stress conditions. A sensitivity analysis with respect to hardening and damage parameters is carried out to identify the most influential parameters on strain localization predictions.

Keywords: Strain localization, bifurcation analysis, ductile damage, thin sheet metals.

INTRODUCTION

The concept of Forming Limit Diagram (FLD) is one of the most common tools used to characterize the formability of sheet metals. The experimental determination of the FLD was first introduced by Keeler (1963). However, this experimental approach turned out to be time consuming, and involving non-negligible costs. Alternatively, FLDs can be predicted by finite element simulations, using various sheet metal forming processes (e.g., Nakazima test, Marciniak test, bulge test, etc.). In such numerical approaches, the accurate determination of FLDs requires coupling of a predictive localization criterion to an appropriate constitutive law with reliable material parameters. The latter must be identified at sufficiently large deformations (i.e., of the same order of magnitude as necking strains).

Several theoretical and numerical approaches have been developed in the literature to predict the occurrence of localized necking in thin sheet metals. The Marciniak–Kuczyński approach (M–K) is the most adopted localized necking criterion for the determination of FLDs for sheet metals (Marciniak, 1967). It is based on the existence of an initially defective region, with an initial geometric or material imperfection, from which localized necking may initiate (see, e.g., Marciniak, 1967; Yamamoto, 1978). Another family of localized necking criteria is founded on bifurcation theory, and has been developed to predict strain localization in the form of shear band or localized necking (see, e.g., Hill, 1952; Rudnicki, 1975; Rice, 1976; Bigoni, 1991; Neilson, 1993). In contrast to the M–K approach, the bifurcation analysis does not require the introduction of arbitrarily user-defined parameters. However, it requires considering softening behavior, which may be introduced by coupling with damage. For the latter, two major theories have been developed in the literature, in the past few decades, to model the initiation and evolution of ductile damage. The first theory is based on a micromechanical analysis of void growth, which describes the ductile damage mechanisms in

porous materials. It has been initiated by Gurson (1977), modified by Tvergaard and Needleman (Tvergaard, 1981; 1984), and subsequently improved by a number of contributors (Rousselier, 1987; Pardoen, 1998; Benzerga, 2001; Monchiet, 2008). The second theory, known as continuum damage mechanics (see, e.g., Lemaitre, 1992; Chaboche, 1999), is based on the introduction of a damage variable, which represents the surface density of defects, and can be modeled as isotropic scalar variable (Lemaitre, 1985; Chaboche, 2006), or tensor variable for anisotropic damage (Chow, 1989; Chaboche, 1993; Abu Al-Rub, 2003).

In this work, an elastic–plastic constitutive model, with Hill (1948) anisotropic plastic yield surface, is coupled with the Lemaitre isotropic damage approach. This fully coupled elastic–plastic–damage model is combined with the Rice bifurcation criterion (Rice, 1976) to predict the occurrence of localized necking in thin sheet metals. The resulting numerical tool is implemented into the finite element code ABAQUS, within the large-strain framework and plane-stress conditions. The material parameters associated with the fully coupled elastic–plastic–damage model are identified based on tensile tests, using an inverse identification procedure. A sensitivity study is conducted with respect to material parameters in order to identify the most influential parameters on the development of necking. The paper emphasizes the importance of identifying reliable material parameters for accurate prediction of FLDs.

CONSTITUTIVE EQUATIONS

In this work, an anisotropic elastic–plastic model is fully coupled with the continuum damage mechanics approach (Lemaitre, 1985), in which damage is introduced as an isotropic scalar variable d ($0 \le d \le 1$), which represents the surface density of microcracks. Using the strain equivalence principle (Lemaitre, 1992), the Cauchy stress tensor $\boldsymbol{\Sigma}$ is related to the effective stress $\tilde{\boldsymbol{\Sigma}}$ of the equivalent undamaged material as follows:

$$\tilde{\boldsymbol{\Sigma}} = \frac{\boldsymbol{\Sigma}}{1-d} \,. \tag{1}$$

By replacing the rate form of Eq. (1) in the hypo-elastic law for the effective stress, the Cauchy stress rate tensor can be expressed as

$$\dot{\boldsymbol{\Sigma}} = (1-d)\,\mathbf{C} : \left(\mathbf{D} - \mathbf{D}^{\mathrm{p}}\right) - \frac{\dot{d}}{1-d}\boldsymbol{\Sigma} \,, \tag{2}$$

where $\mathbf{C}$ is the fourth-order elasticity tensor, while $\mathbf{D}$ and $\mathbf{D}^{\mathrm{p}}$ are the strain rate tensor and plastic strain rate tensor, respectively.

By considering the normality law for the plastic flow rule, the plastic strain rate tensor $\mathbf{D}^{\mathrm{p}}$ is obtained as

$$\mathbf{D}^{\mathrm{p}} = \dot{\gamma}\,\tilde{\mathbf{P}} \,, \tag{3}$$

where $\tilde{\mathbf{P}} = \partial\Phi / \partial\boldsymbol{\Sigma}$ is the flow direction, normal to the yield surface defined by the potential Φ, and $\dot{\gamma}$ is the plastic multiplier.

The conditions of plastic loading / elastic unloading, which involve the plastic yield function and the internal state variables, can be written in the Kuhn–Tucker form

$$\Phi = \Sigma_{eq}\left(\tilde{\boldsymbol{\Sigma}}', \mathbf{X}\right) - \Sigma_{Y} \le 0 \quad ; \quad \dot{\gamma} \ge 0 \quad ; \quad \dot{\gamma}\Phi = 0 \,, \tag{4}$$

where $\Sigma_{eq} = \sqrt{(\tilde{\boldsymbol{\Sigma}}' - \mathbf{X}) : \mathbf{M} : (\tilde{\boldsymbol{\Sigma}}' - \mathbf{X})}$ is the equivalent stress, and $\tilde{\boldsymbol{\Sigma}}'$ is the deviatoric part of the effective stress. The fourth-order tensor $\mathbf{M}$ contains the six anisotropy coefficients associated with the Hill (1948) quadratic yield criterion. For the studied material, the contribution to isotropic hardening is characterized by the size of the yield surface Σ_Y, while kinematic hardening is represented by the back-stress tensor $\mathbf{X}$.

Using the consistency condition $\dot{\Phi} = 0$, together with the above equations, the expression of the plastic multiplier $\dot{\gamma}$ can be written as

$$\dot{\gamma} = \frac{1}{H_\gamma} \mathbf{P} : \mathbf{C} : \mathbf{D}, \tag{5}$$

where $\mathbf{P} = (1-d)\tilde{\mathbf{P}}$, and H_γ is a scalar modulus given by

$$H_\gamma = \mathbf{P} : \mathbf{C} : \tilde{\mathbf{P}} + \mathbf{P} : \mathbf{H}_\mathbf{X} + H_\Sigma. \tag{6}$$

In the equation above, the second-order tensor $\mathbf{H}_\mathbf{X}$ represents the kinematic hardening modulus, which is used to describe the evolution of the back-stress tensor $\mathbf{X}$ (i.e., $\dot{\mathbf{X}} = \mathbf{H}_\mathbf{X}\, \dot{\gamma}$), while H_Σ is the scalar isotropic hardening modulus (i.e., defined such that $\dot{\Sigma}_Y = H_\Sigma\, \dot{\gamma}$).

To derive the stress–strain relationship under the following rate form:

$$\dot{\boldsymbol{\Sigma}} = \mathbf{C}^{ep} : \mathbf{D}, \tag{7}$$

the plastic multiplier $\dot{\gamma}$ derived in Eq. (5) is substituted in the hypo-elastic law (Eq. (2)). Accordingly, the analytical elastic–plastic tangent modulus $\mathbf{C}^{ep}$, which relies the Cauchy stress rate to the strain rate, is derived as follows:

$$\mathbf{C}^{ep} = (1-d)\mathbf{C} - \alpha \left(\frac{(\mathbf{C} : \mathbf{P}) \otimes (\mathbf{P} : \mathbf{C})}{H_\gamma} + \frac{H_d \tilde{\boldsymbol{\Sigma}} \otimes (\mathbf{P} : \mathbf{C})}{H_\gamma} \right), \tag{8}$$

where $\alpha = 1$ for plastic loading and $\alpha = 0$ otherwise, while H_d is a scalar modulus defining the damage evolution (i.e., such that $\dot{d} = H_d\, \dot{\gamma}$), which will be explicitly described later. In this work, kinematic hardening is not considered (i.e., $\mathbf{H}_\mathbf{X} = \mathbf{0}$ in Eq. (6)), and isotropic hardening is described by the following Swift law:

$$\Sigma_Y = k \left(\varepsilon_0 + \bar{\varepsilon}^p \right)^n \tag{9}$$

where k, ε_0 and n are hardening-related material parameters, and $\bar{\varepsilon}^p$ is the equivalent plastic strain.

Finally, the evolution law for the damage variable is expressed by the following equation (see, e.g., Lemaitre, 1992; Haddag, 2009):

$$\dot{d} = H_d\, \dot{\gamma} = \begin{cases} \dfrac{1}{(1-d)^\beta} \left(\dfrac{Y_e - Y_{ei}}{S} \right)^s \dot{\gamma} & \text{if} \quad Y_e \geq Y_{ei} \\ 0 & \text{otherwise} \end{cases}, \tag{10}$$

where Y_e is the elastic strain energy density release, and (β, S, s, Y_{ei}) are damage-related material parameters.

LOCALIZED NECKING CRITERION

The fully coupled elastic–plastic–damage model described by the above constitutive equations is combined in this work with the bifurcation approach (see Rudnicki, 1975; Rice, 1976), in order to predict the occurrence of localized necking in sheet metals. The adopted necking criterion is based on bifurcation theory, in which the localization of deformation in the form of a narrow band (see Fig.1) corresponds to loss of uniqueness for the solution of the rate equilibrium equations. In other words, the onset of localized necking is viewed as a transition from a homogeneous state of deformation towards a heterogeneous one, corresponding to a discontinuity in the velocity gradient.

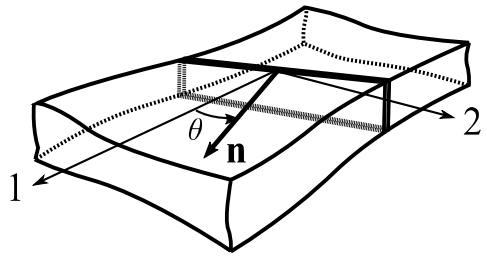

Fig. 1 - Schematic illustration of a localization band

Introducing the nominal stress tensor $\mathbf{N}$, the constitutive equation can be expressed within the large-strain framework as follows:

$$\dot{\mathbf{N}} = \mathbf{L} : \mathbf{G}\,, \tag{11}$$

where $\mathbf{G}$ is the velocity gradient, and $\mathbf{L}$ is the fourth-order tangent modulus given by

$$\mathbf{L} = \mathbf{C}^{ep} + \mathbf{T}_1 - \mathbf{T}_2 - \mathbf{T}_3\,, \tag{12}$$

with $\mathbf{T}_1$, $\mathbf{T}_2$, and $\mathbf{T}_3$ fourth-order tensors containing Cauchy stress components. Their expressions write (see Haddag, 2009)

$$\begin{cases} \mathrm{T}_{1ijkl} = \Sigma_{ij}\delta_{kl} \\ \mathrm{T}_{2ijkl} = \dfrac{1}{2}\left(\delta_{ik}\Sigma_{lj} + \delta_{il}\Sigma_{kj}\right) \\ \mathrm{T}_{3ijkl} = \dfrac{1}{2}\left(\Sigma_{ik}\delta_{lj} - \Sigma_{il}\delta_{jk}\right) \end{cases}. \tag{13}$$

At the occurrence of a localization band, which is defined by its normal $\mathbf{n}$ (see Fig. 1), the continuity of the nominal stress rate vector across the discontinuity surfaces can be written as

$$\mathbf{n} \cdot \left[\!\left[\dot{\mathbf{N}} \right]\!\right] = \mathbf{0}\,, \tag{14}$$

where $[\![\dot{\mathbf{N}}]\!] = \dot{\mathbf{N}}^{+} - \dot{\mathbf{N}}^{-}$ denotes the jump in the nominal stress rate across the localization band planes. Using Maxwell's compatibility condition, the jump in the velocity gradient can be written in the following form:

$$[\![\mathbf{G}]\!] = \boldsymbol{\lambda} \otimes \mathbf{n}, \tag{15}$$

where vector $\boldsymbol{\lambda}$ defines the localization bifurcation mode (e.g., shear mode when $\boldsymbol{\lambda} \perp \mathbf{n}$). By combining equations (11), (14) and (15), the critical condition, which corresponds to the loss of ellipticity of the associated boundary value problem, can be derived for a non-trivial solution for vector $\boldsymbol{\lambda}$, and writes (Rice, 1976)

$$\det \mathbf{A} = \det(\mathbf{n} \cdot \mathbf{L} \cdot \mathbf{n}) = 0, \tag{16}$$

where $\mathbf{A}$ is the so-called acoustic tensor.

The above loss of ellipticity condition is numerically solved by computing the determinant of the acoustic tensor $\mathbf{A}$ for each loading increment. The numerical detection of localized necking is achieved when the minimum of the determinant of the acoustic tensor $\mathbf{A}$, over all possible normal vectors to the localization band, becomes non-positive.

NUMERICAL RESULTS AND DISCUSSIONS

The proposed approach, which consists in combining the fully coupled elastic–plastic–damage model with the bifurcation-based localization criterion, is implemented into the finite element code ABAQUS, within the framework of large plastic strains and plane-stress conditions. This approach is applied in this work to the prediction of localized necking in sheet metals subjected to in-plane biaxial loading.

Identification of the material parameters

The material considered in this work is an AA6016-T4 aluminum alloy sheet, which is modeled using the constitutive equations described above, in conjunction with the Swift isotropic hardening law. The Hill'48 anisotropy coefficients are determined using the three values of Lankford's coefficients r_0, r_{45} and r_{90} obtained from uniaxial tensile tests performed on rectangular specimens cut at 0°, 45° and 90°, respectively, with respect to the rolling direction. The Swift hardening parameters have been identified by Kami (2015) using an inverse identification procedure based on the least squares method and experimental hardening curves. The associated anisotropy coefficients and hardening parameters are summarized in Tables 1 and 2, respectively.

Table 1 - Hill'48 anisotropy coefficients for AA6016 aluminum taken from Kami (2015)

Hill'48 coefficients	F	G	H	L	M	N
Value	0.647705	0.643956	0.356043	1.5	1.5	1.174250

Table 2 - Swift's hardening parameters for AA6016 aluminum taken from Kami (2015)

Material	k [MPa]	ε_0	n
AA6016-T4	525.77	0.011252	0.2704

The damage parameters associated with the Lemaitre model are identified using a numerical inverse identification procedure based on simulated and experimental load–displacement responses of a standard tensile test. The identified damage parameters are summarized in Table 3.

Table 3 - Identified damage parameters for AA6016 aluminum

β	S	s	Y_{ei}
12	4	1.3	0

Figure 2 compares the simulated load–displacement response for the tensile test, which is obtained using the above identified parameters, to the experimental one given in Kami (2015). It can be seen that the predicted curve is in good agreement with the experimental data, especially in the softening regime where the sudden drop in the load–displacement response is well reproduced by the proposed fully coupled elastic–plastic–damage model.

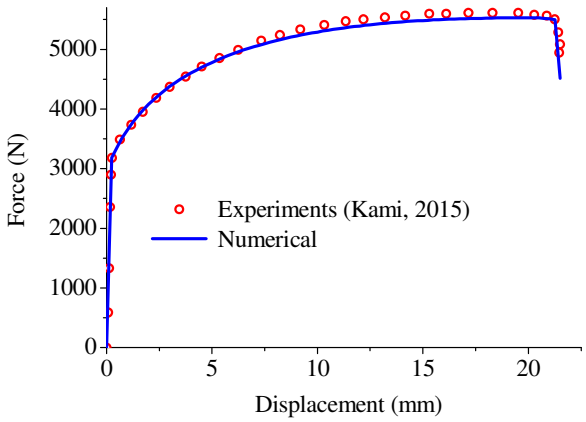

Fig. 2 - Comparison between the simulated and experimental load–displacement response, up to final fracture for the tensile test

Prediction of FLD using the localization bifurcation analysis

In this section, the occurrence of localized necking in the AA6016-T4 aluminum sheet is investigated using the proposed Lemaitre damage–Rice approach. In order to restrict the analysis to only material-type instabilities, the simulations are performed using a single finite element with one integration point (i.e., C3D8R ABAQUS finite element). The material parameters for the AA6016-T4 aluminum sheet are those identified in the previous section (see Tables 1, 2, and 3).The full details regarding the adopted boundary conditions and the procedure used for determining the FLD can be found in Bouktir (2016).

Figure 3 shows the FLD predicted with the present approach along with the experimental FLDs taken from Kami (2015) and Lademo (2009). It can be observed that, in the whole, the FLD predicted with the proposed approach is in good agreement with experiments, especially in the left-hand side of the FLD (strain-path loadings from uniaxial tension (UT) to plane-strain tension (PST)). For the right-hand side of the FLD, the limit strains are well predicted with respect to experiments near the balanced biaxial tension (BBT) loading path, while they are overestimated for the other biaxial tension loading paths.

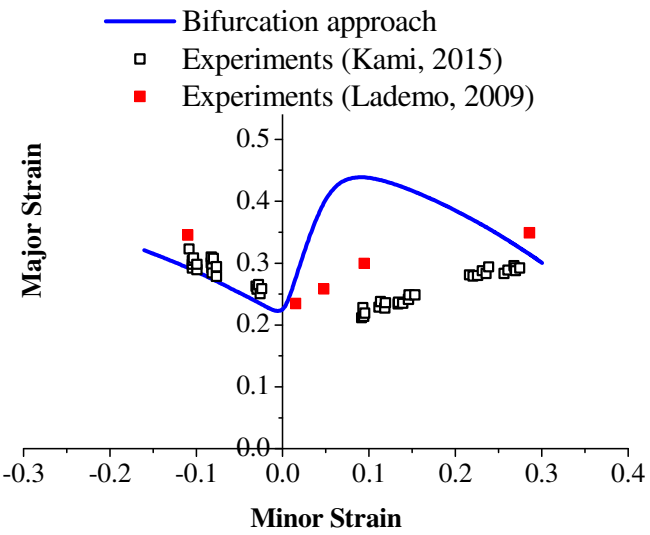

Fig. 3 - Comparison between the FLD predicted with the proposed approach and the experimental FLDs from Kami (2015) and Lademo (2009)

Effect of material parameters on localized necking predictions

In order to identify the most influential parameters on the prediction of FLDs, a sensitivity study with respect to material parameters is conducted in this section. For this purpose, numerical FLDs are determined by varying one parameter at a time, while the remaining parameters are kept to their values reported in Tables 2 and 3. In addition, the effect of material parameters on the load–displacement response for the tensile test is also investigated. For conciseness, only the parametric study with respect to the hardening exponent n and the damage parameter β is reported here.

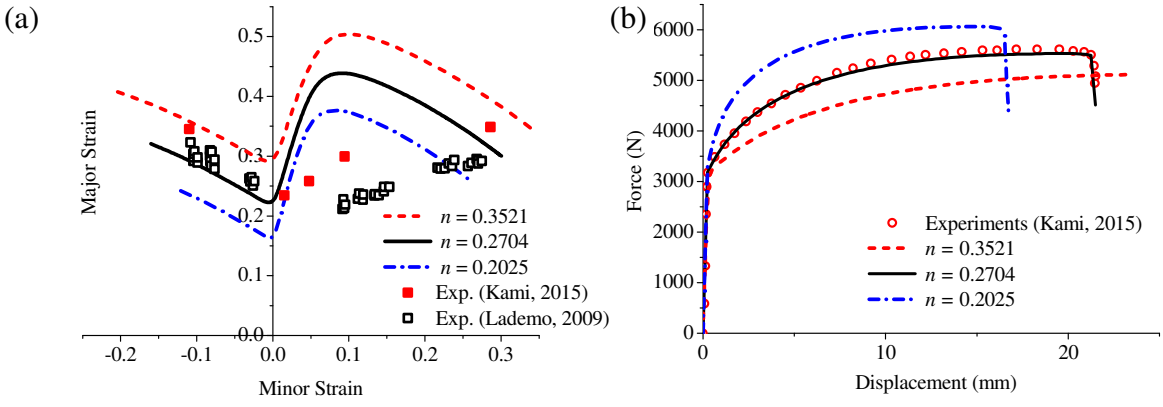

Fig. 4 - Effect of variation of the hardening exponent n on the predictions of (a) the FLD and (b) the load–displacement response for the tensile test

Figure 4 shows the effect of the hardening exponent n on the FLD predictions and on the load–displacement responses for the uniaxial tensile test. It can be seen that increasing the hardening exponent n leads to an increase of all limit strain points of the FLD. Also, this parameter has a significant impact on the entire load–displacement response for the tensile

test. This trend is consistent with the literature findings, where it has been shown that hardening parameters have a non-negligible effect on strain localization (see, e.g., Doghri, 1995; Hora, 1996). Furthermore, the effect of the hardening exponent n on the Cauchy stress–strain curve and on the evolution of damage along the three particular strain paths of UT, PST, and BBT is illustrated in Fig. 5. These figures clearly show the impact of strain hardening on the damage evolution and, thereby, on strain localization.

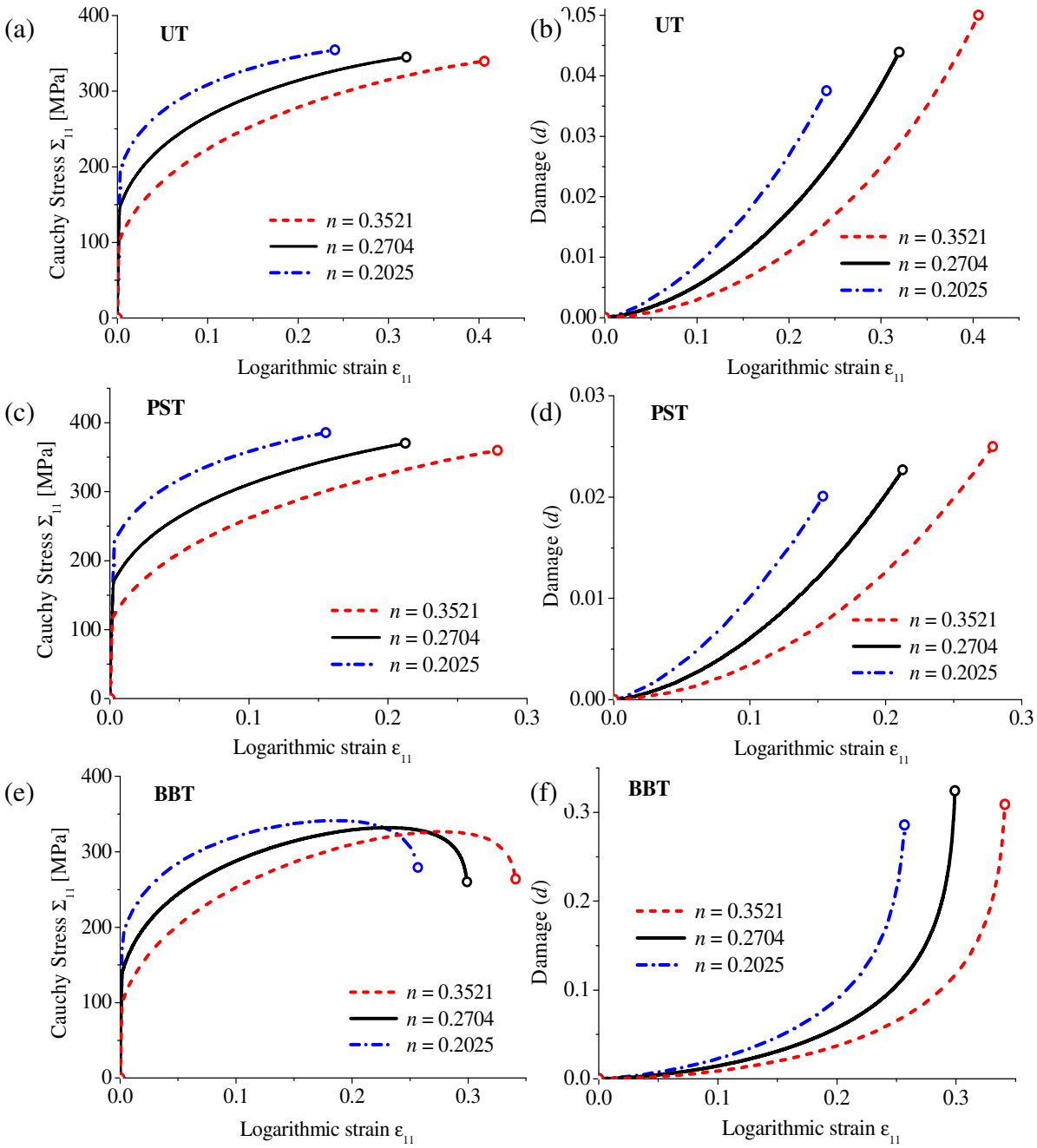

Fig. 5 - Effect of variation of the hardening exponent n on the evolution of the Cauchy stress (left) and damage variable (right) up to localization, along the UT, PST, and BBT strain paths

Figure 6 shows the effect of varying the damage parameter β on the FLD predictions and on the load–displacement responses corresponding to the uniaxial tensile test for the studied material. It can be seen that the damage parameter β has a small effect on the left-hand side of the FLD, while its effect is significant in the right-hand side of the FLD. These trends are confirmed with the evolution of the Cauchy stress and the damage variable given in Fig. 7 along the particular strain paths of UT, PST, and BBT. In this figure, it is revealed that the damage level at localization is small for the UT and PST strain paths (less than 5% and 3%, respectively), compared to that found for the BBT strain path (around 40%). In the latter, both the hardening and damage parameters have a significant impact on strain localization, while for the UT and PST strain paths, only hardening parameters play a key destabilizing role in triggering plastic flow localization. Furthermore, the load–displacement response (see Fig. 6(b)), which corresponds to the UT strain path, is not affected by the variation of the damage parameter β in the range of uniform elongation, i.e. before the onset of diffuse necking, corresponding to the maximum load point (see Considère, 1885). In the softening regime, starting from the maximum load point and up to final fracture, the damage parameter β has a slight effect on the load–displacement response for the uniaxial tensile test, which makes it difficult to properly identify this parameter in the post-necking range. Consequently, several values for the damage parameter β are potentially possible, leading to a non-negligible error on the prediction of the FLD. These results suggest incorporating several mechanical tests, involving various strain paths, in the identification procedure in order to improve the reliability of the material parameters and, in particular, damage-related parameters.

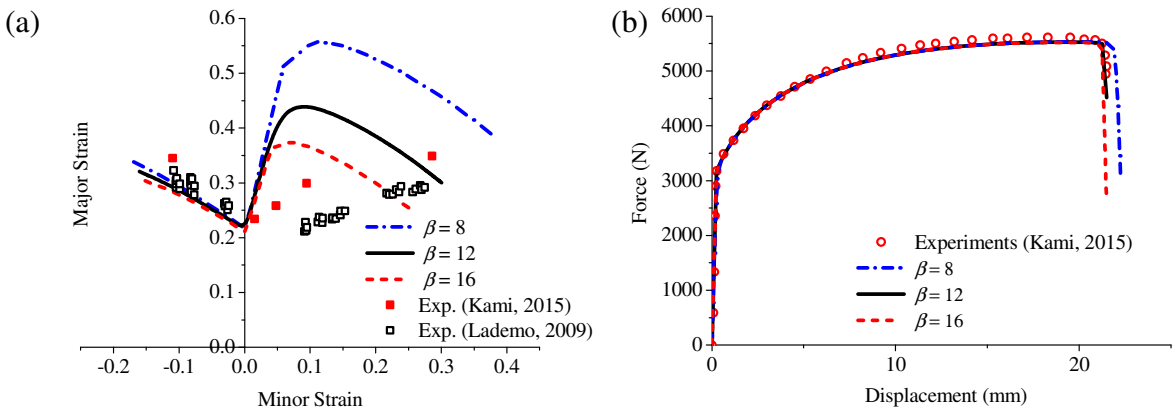

Fig. 6 - Effect of variation of the damage parameter β on the predictions of (a) the FLD and (b) the load–displacement response for the tensile test

CONCLUSION

In this work, a fully coupled anisotropic elastic–plastic model with the Lemaitre damage theory has been combined with Rice's bifurcation criterion, in order to predict the occurrence of localized necking in AA6016-T4 aluminum sheet. The resulting approach has been implemented into the finite element software ABAQUS/Standard, within the framework of large strains and plane-stress conditions. The damage parameters have been first identified using an inverse identification procedure based on uniaxial tensile tests. Then, the identified parameters have been used to predict the FLD of the AA6016-T4 aluminum sheet, based on

the proposed approach. The obtained FLD showed good agreement with the experimental results. A parametric study with respect to strain hardening and damage parameters has been conducted in order to identify the most influential material parameters on strain localization. This study revealed that strain hardening has a significant impact on strain localization, which is consistent with the literature findings. As to damage parameters, the latter showed a small effect on the left-hand side of the FLD, as well as on the load–displacement response for the uniaxial tensile test, while their impact on the right-hand side of the FLD was found significant. This work emphasizes the importance of the mechanical tests used in the identification procedure in order to determine reliable material parameters and, thus, accurate predictions for the FLDs.

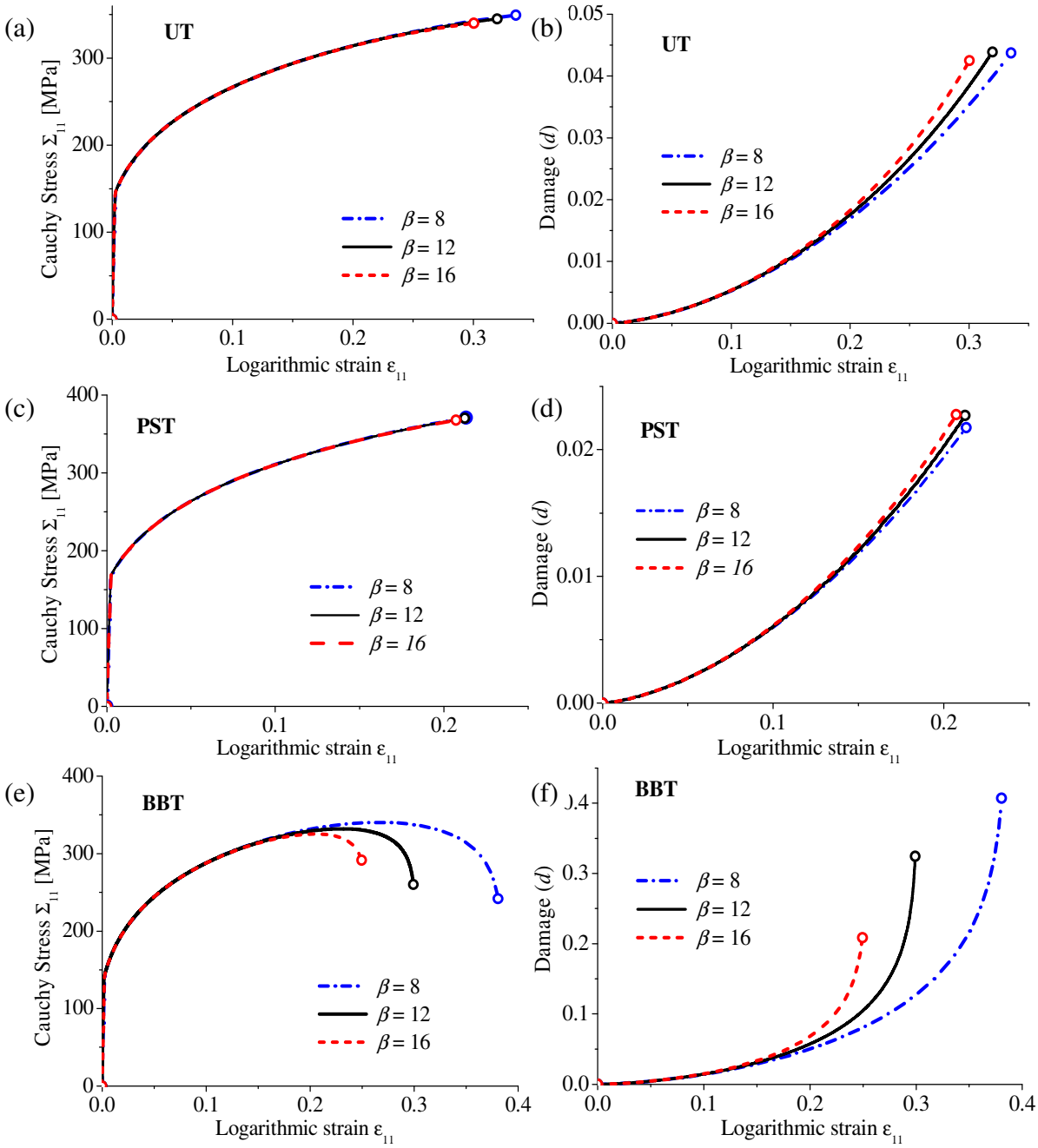

Fig. 7 - Effect of variation of the damage parameter β on the evolution of the Cauchy stress (left) and damage variable (right) up to localization, along the UT, PST, and BBT strain paths

REFERENCES

Abu Al-Rub RK, Voyiadjis GZ. On the coupling of anisotropic damage and plasticity models for ductile materials. International Journal of Solids and Structures, 2003, 40, p. 2611–2643.

Benzerga AA, Besson J. Plastic potentials for anisotropic porous solids. European Journal of Mechanics - A/Solids, 2001, 20, p. 397–434.

Bigoni D, Hueckel T. Uniqueness and localization - I. associative and non-associative elastoplasticity. International Journal of Solids and Structures, 1991, 28, p. 197–213.

Bouktir Y, Chalal H, Haddad M, Abed-Meraim F. Investigation of ductility limits based on bifurcation theory coupled with continuum damage mechanics. Materials and Design, 2016, 90, p. 969–978.

Chaboche JL. Development of continuum damage mechanics for elastics solids sustaining anisotropic and unilateral damage. Int. J. Damage Mech., 1993, 2, p. 311–329.

Chaboche JL. Thermodynamically founded CDM models for creep and other conditions: CISM courses and lectures No 399, International Centre for Mechanical Sciences. Creep Damage Mater. Struct., 1999, p. 209–283.

Chaboche JL, Boudifa M, Saanouni M. A CDM approach of ductile damage with plastic compressibility. International Journal of fracture, 2006, 137, p. 51–75.

Chow CL, Lu TJ. On evolution laws of anisotropic damage. Engineering Fracture Mechanics, 1989, 34, p. 679–701.

Considère A. Mémoire sur l'emploi du fer et de l'acier dans les constructions. Annals des Ponts et Chaussées, 1885, 9, p. 574.

Doghri I, Billardon R. Investigation of localization due to damage in elasto-plastic materials. Mechanics of Materials, 1995, 19, p. 129–149.

Gurson AL. Continuum theory of ductile rupture by void nucleation and growth: Part I - Yield criteria and flow rules for porous ductile media. J. Eng. Mater. Technol., 1977, 99, p. 2–15.

Haddag B, Abed-Meraim F, Balan T. Strain localization analysis using a large deformation anisotropic elastic–plastic model coupled with damage. International Journal of Plasticity, 2009, 25, p. 1970–1996.

Hill R. A theory of the yielding and plastic flow of anisotropic metals. Proc. Royal Soc., 1948, A 193, p. 281–297.

Hill R. On discontinuous plastic states, with special reference to localized necking in thin sheets. Journal of the Mechanics and Physics of Solids, 1952, 1, p. 9–30.

Hora P, Tong L, Reissner J. A prediction method of ductile sheet metal failure in FE simulation. Proceedings of Numisheet, 1996, p. 252–256.

Kami A, Dariani BM, Vanini AS, Comsa DS, Banabic D. Numerical determination of the forming limit curves of anisotropic sheet metals using GTN damage model. Journal of Materials Processing Technology, 2015, 216, p. 472–483.

Keeler S, Backofen WA. Plastic instability and fracture in sheets stretched over rigid punches. ASM Trans. Q., 1963, 56, p. 25–48.

Lademo OG, Engler O, Keller S, Berstad T, Pedersen KO, Hopperstad OS.Identification and validation of constitutive model and fracture criterionfor AlMgSi alloy with application to sheet forming. Materials and Design, 2009, 30, p. 3005–3019.

Lemaitre J. A continuous damage mechanics model for ductile fracture. Journal of Engineering Materials and Technology, 1985, 107, p. 83–89.

Lemaitre J. A course on damage mechanics. Springer-Verlag, Berlin, Heidelberg, 1992.

Marciniak Z, Kuczyński K. Limit Strains in the Processes of Stretch-Forming Sheet Metal. International Journal of Mechanical Sciences, 1967, 9, p. 613–620.

Monchiet V, Cazacu O, Charkaluk E, Kondo D. Macroscopic yield criteria for plastic anisotropic materials containing spheroidal voids. International Journal of Plasticity, 2008, 24, p. 1158–1189.

Neilsen MK, Schreyer HL. Bifurcations in elastic–plastic materials. International Journal of Solids and Structures, 1993, 30, p. 521–544.

Pardoen T, Doghri I, Delannay F. Experimental and numerical comparison of void growth models and void coalescence criteria for the prediction of ductile fracture in copper bars. Acta Mater., 1998, 46, p. 541–552.

Rice JR. The localization of plastic deformation. In: theoretical and applied mechanics, 14th Inter. Congress on Theor. Appl. Mech., Delft, Netherlands, 1976, p. 207-220.

Rousselier G. Ductile fracture models and their potential in local approach of fracture. Nuclear Engineering and Design, 1987, 105, p. 97–111.

Rudnicki, JW, Rice JR. Conditions for the localization of deformation in pressure sensitive dilatant materials. Journal of the Mechanics and Physics of Solids, 1975, 23, p. 371–394.

Tvergaard V. Influence of voids on shear band instabilities under plane strain conditions. International Journal of Fracture, 1981, 17, p. 389–407.

Tvergaard V, Needleman A. Analysis of the cup-cone fracture in a round tensile bar. Acta Metall., 1984, 32, p. 157–169.

Yamamoto H. Conditions for shear localization in the ductile fracture of void-containing materials. International Journal of Fracture, 1978, 14, p. 347–365.